Design of a Fracture Detection System based on Deep Program in a Convolutional Neural Network

Payman Hussein Hussan
Babylon Technical Institute, Al-Furat Al-Awsat Technical University, Kufa, Iraq.
E-mail: inb.Beman10@atu.edu.iq

Syefy Mohammed Mangj Al-Razoky
Babylon Technical Institute, Al-Furat Al-Awsat Technical University, Kufa, Iraq.

Hasanain Mohammed Manji Al-Rzoky
Directorate Education of Babylon, Ministry of Education, Iraq.

Received April 07, 2021; Accepted August 02, 2021
ISSN: 1735-188X
DOI: 10.14704/WEB/V18I2/WEB18336

Abstract

This paper presents an efficient method for finding fractures in bones. For this purpose, the pre-processing set includes increasing the quality of images, removing additional objects, removing noise and rotating images. The input images then enter the machine learning phase to detect the final fracture. At this stage, a Convolutional Neural Networks is created by Genetic Programming (GP). In this way, learning models are implemented in the form of GP programs. And evolve during the evolution of this program. Then finally the best program for classifying incoming images is selected. The data set in this work is divided into training and test friends who have nothing in common. The ratio of training data to test is equal to 80 to 20. Finally, experimental results show good results for the proposed method for bone fractures.

Keywords

Deep Learning, Computer-aided Diagnosis (CAD), Genetic Programming (GP), Convolutional Neural Networks.

Introduction

New trends and technology in radiology have advanced the diagnosis and treatment of many diseases (Ismael et al., 2020). However, the number of patients and radiology images stands 7.5 times the number of radiologists per year. Because all of these images need to be examined, the detection process must be performed at the shortest possible time (Li et al., 2020). The analysis of medical images is a highly specialized, challenging, and error-prone action that depends on the experience of radiologists (Ismael et al., 2020). However, radiologists may fail to accurately interpret images in some cases due to the excessive work

volume per day. Oftentimes, in the absence of orthopedic specialists in the emergency center, the rate of such errors may rise by about 41 to 80 percent. Misdiagnosis can adversely affect subsequent performance during the patient's therapy plans (Lindsey et al., 2018). In recent years, computer-aided diagnosis (CAD) has been proposed in order to diminish the rate of such problems and achieve higher diagnosis efficiency (Guan et al, 2019), where physicians can rely on them as a second opinion to assist and support their decisions. Many studies have been carried out to design CADs for application in various medical settings such as diagnosis of cancer, breast lesions, brain tumor, and especially bone fractures.

CAD systems can be classified into two categories in terms of feature extraction purposes, i.e., the hand-craft feature extraction and feature extraction using deep learning. In the first category and before generating a feature, a proper feature must be identified by an expert and then extracted by hand-craft technique (Al-Masni et al., 2018). The most important of these features include contrast, correlation, energy, homogeneity, mean, variance, standard deviation (SD), correlation, Gabor orientation (GO), and Markov Random Field (MRF) (Prihatini et al., 2017).

There are two main challenges with the first category, i.e., these methods fail to show a great performance, and generating hand-crafted features requires the environmental knowledge of the expert. Recently, researchers have shifted toward feature extraction using deep learning. Today, machine learning and deep learning can improve the efficiency of conventional CAD systems by overcoming the constraints discussed above (Guan et al., 2020).

Some algorithms can be designed using deep learning techniques that accurately perform visual tasks (e.g., dimension recognition, localization, and classification), learn a set of prominent features from the entire data, and show high cognitive accuracy by substituting them with hand-crafted features (Bi et al., 2019). Many studies have been carried out using deep learning in medical settings that have achieved remarkable achievement. For example, convolutional neural networks (CNNs) have been applied in cancer prediction, detection of brain tumor division, brain image analysis, pulmonary nodule detection, and wrist fracture diagnosis (Raghavendra et al., 2018).

This work attempts to propose an efficient system for rapid and accurate diagnosis of bone fractures using GP-based CNN, according to data obtained from X-ray images. The general framework of the proposed system compromises three phases of bone tissue extraction, feature production, and classification of fractures. This was performed by gathering a set of X-ray images, which includes four classes of normal bones, fractured bones, skeletal bones,

and bones with other anomalies. Data were divided into two training and validation categories with a ratio of 20 to 80 according to the Pareto principle. Experiments showed the acceptability of the detection results of the proposed algorithm.

Proposed Method

The Proposed GP-based CNN

The proposed method is composed of three phases:

1. Extraction of bone tissue
2. Feature generation
3. Classification of fractures

In the preprocessing phase, the two top and bottom points of the input image are first identified upon raising the image contrast and eliminating noise. The points obtained will be used in the next two preprocessing steps. The specified points are first connected by a line (Umadevi et al., 2012). The image rotates then according to the angle of the drawn line. In the second phase, the bone tissue area is separated from the image using the coordinates of the obtained points. In the feature generation phase, the proposed CNN3 is used. The input to CNN3 is a resized image of bone tissue and the output is a feature vector. The last step is to use the SVM classification algorithm to diagnose the type of bone fracture based on the generated feature. Finally, in the testing phase, the performance and contents of the proposed system are evaluated (Wang et al., 2016; Korfiatis et a., 2017). These steps are discussed in detail in the following sections. The schematic diagram of the proposed system is shown in figure 1.

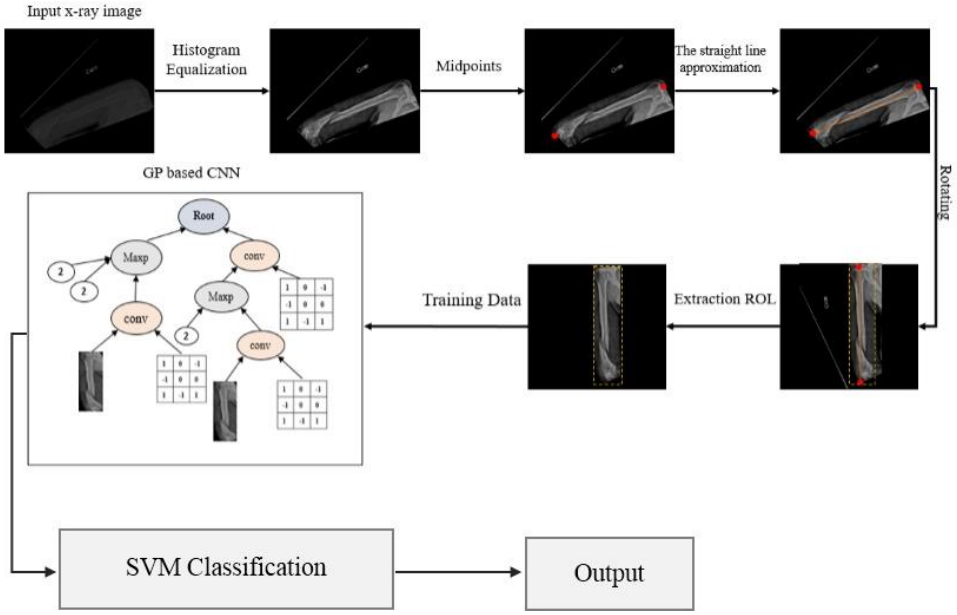

Figure 1 The process of detecting fracture in the proposed method

Image Preprocessing

We are facing two obstacles when using X-ray images in the MURA dataset, i.e., the presence of noise and the dark background of the images (Al-Ayyoub et al., 2013). Therefore, image processing methods should be used to solve these two problems. Morphological methods have been used to diminish the influences of image noise. The isolated noise in the image can be eliminated and the main area of the image can be identified using the opening operation. Here the main area of the image refers to all the bones and fractures. Histogram equalization is used to increase the brightness of the image, aiming to perform a gray stretch on the original image (Ho et al., 2017). The number of gray levels of the output image is 256. The use of these two processes improves the contrast of the image and helps to achieve the clearest fracture area in the final image (Umadevi et al., 2012). The effect of histograms on increasing resolution and improving image quality is shown in Figure 2.

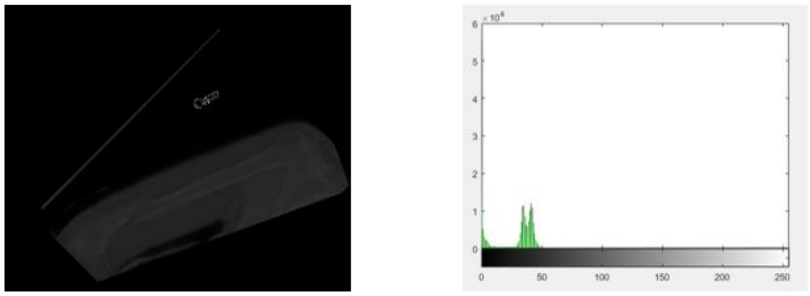

a. Original Image

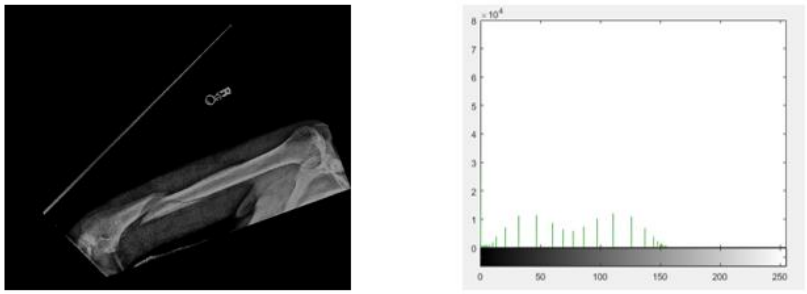

b. Histogram Equalization Image

Figure 2 The impact of the histogram on increasing the resolution and improving the quality of the image

The next step is to extract the bone tissue from the improved images. The first process is to extract the ROI of bone tissue. For this, the midpoints at both the beginning and end of the bone must first be calculated using a convex bull (Korfiatis et al., 2017). The obtained points are then connected by drawing a direct line. The ROI of the target area must be obtained in order to extract bone tissue. First, the enhanced image will be binary by specifying a certain

threshold. Then, all the objects in the black and white image are identified with the help of image processing functions. The area of interest, which is the bone tissue, is assuredly the largest object, i.e., a continuous surface in the image. Therefore, other unnecessary areas will be removed from the image margin using Equation (1). Finally, by drawing a box, the area of bone tissue specified in the binary image is isolated from the background. Using the convex bull, the coordinates of the points in the four corners of the box are specified, and then the middle of both points in the width of the rectangle is determined as the midpoints (Ebsim et al., 2018). The coordinates of the midpoints and the line drawn between them are used for the next two processes, i.e., rotating process and cropping the image. The next step is to rotate the image to create a vertical image of the bone using the drawn line. The rotation of the line should create an angle of 90 degrees with the x-axis. Images, where the bone is vertical, do not need to be rotated. Ultimately, after rotating the image and verticalizing the straight line, the image should be cropped to allow the bone tissue to be isolated from the background. The upper and lower boundaries of the bone are adjusted using the coordinates of the points obtained in the previous steps, and the left and right boundaries of the bone are determined using the x coordinates on the line drawn. Following the extraction of the bone tissue, images of different sizes are obtained that must be resized to the same size. Hence the training and test data sets are altered by 30 × 80 pixels.

a **b** **c**

Figure 3 Rotate bone images

Feature Generation Using GP-based CNN

In this section, the features of GP-based CNN used in the proposed method are described, including the structure of GP genes, the set of functions used, and the terminals used to build the CNN tree (Tomita et al., 2018).

1. Gene Structure

In general, the GPCNN method works as follows. The proposed method starts by randomly generating multiple GP trees with new terminals. The structure of these trees is based on STGP, which, unlike conventional models, provides one type of input and one type of

output for each function and one type of output for each terminal. Each feature vector extracted is classified by a vector machine (SVM) (Yamada et al., 2016; Gao et al., 2018).

The GPCNN consists of several layers including an input layer, a convolution, a pooling layer, a convolution/pooling layer, a concatenation layer, and an output layer. Each layer has a different function, which is introduced in the following section. First, the input layer receives x-ray images. The convolution layer performs the convolution operation and further has several critical functions for rescaling, activation, or enhancement. The convolution/pooling layer works similar to the convolution and pooling layers. The pooling layer performs max pooling operations to reduce the size of the images. The task of the concatenation layer is to merge two input images. The last layer works to return the attribute vector as an output. As discussed, the input for GPCNN is an image and the output is a feature vector. The dimensions of the feature vector are flexible and not predetermined (Al-Ayyoub et al., 2013; Qadir et al., 2018).

Figure 4 The GPCNN plan

2. Function Set

The functions used in the GP program structure are given in Table 1. The convolution layer includes the functions Conv, Sub, Add, ReLU, Sqrt, and Abs. The conv function uses the evolved filter to perform convolution operations on the input x-ray images.

$$(f * g)(x) = \int_{R^d} f(y)g(x-y)\,dy = \int_{R^d} f(x-y)g(y)dy$$

The sub and add functions perform the weighted addition and subtraction of two images with weights n1 and n2. The two input images may have different sizes. Therefore, the images are cut using the stated functions so that both images reach the same size.

The ReLU, Sqrt, and Abs functions are used to alter image values and modify the numerical space of the sample. In newer networks, it is superior to use ReLU for hidden layers instead of the Sigmoid activator function for two reasons. First, it is simpler and easier to use, and secondly, it does not deal with the problem of the local minimum. In this function, if the

value of X is greater than zero, the output is X, and if the value of X is less than or equal to zero, the output is zero. The ReLU function has a fixed derivative for all inputs greater than zero. This fixed derivative accelerates network learning.

$$F(x) = \max(x, 0)$$

The Concat1, Concat2, Concat3, and Concat4 functions are used in the concatenation layer, which receives multiple images as input and displays them as a vector at the output.

The MaxP function performs a down sampling operation on the input image. This function can reduce the size of the received image, and makes feature extraction operations easier.

3. Classification with SVM

The proposed GPCNN method turns each image into a distinctive feature set. Support Vector Machine (SVM) with the RBF kernel function is used to classify these extracted features. The following equation is also used to evaluate and calculate the GPCNN error rate (Wang et al., 2016).

$$\mathbf{MSE} = \frac{1}{n} \sum_{i=1}^{n} (Y_i - \hat{Y_i})^2$$

Using the SVM classifier with the CNN tree allows creating a lightweight model quickly and efficiently, which is tested on test specimens.

Experiment Design

We have conducted a series of tests to determine the performance of the proposed GPCNN method. In this section, the data set, comparison methods, and parameter settings are fully described.

1. Data Set

In this section, the proposed method will be evaluated on the MURA-v1.1 dataset. This institutional review includes images identified and compatible with HIPAA collected from Stanford hospital's picture archiving and communication system (PACS). Musculoskeletal radiographs include 14,982 studies collected from 12,251 patients, for a total of 40,895 multi-index radiographs. Each of them belongs to one of the seven standard types of radiographic studies of the following limbs: elbow, finger, arm, hand, arm bone, shoulder, and wrist (Wang et al., 2020).

Table 1 summarizes the distribution of normal and abnormal studies.

- **Education (11,255 patients, 13,565 studies, 37,111 images)**
- **Validation (788 patients, 1,208 studies, 3,225 images)**
- **Test (208 patients, 209 studies, 559 images)**

Table 1 Distribution of normal and abnormal studies

Study	Normal	Abnormal	Total
Elbow	1203	768	1971
Finger	1389	753	2142
Forearm	677	380	1057
Hand	1613	602	2215
Humerus	411	367	778
Shoulder	1479	1594	3073
Wrist	2295	1451	3746

2. Results and Test Process

The performance of the proposed method on the MURA database is ideally evaluated and compared with other available methods. The results of this evaluation, according to the three evaluation criteria Precision, Recall, and F-measure, are given. Precision means the number of correct samples from the samples that the model has selected as correct. Recall refers to the ratio of the number of correct samples in the entire dataset, which is among the correctly selected samples of the model. The measure is the harmonic mean between Precision and Recall. The accuracy of the proposed method, according to the accuracy criterion for the MURA database is equal.

In this section and for better comparison, we collect the outstanding works related to the MURA database and compare their results. The details and results of the methods related to the MURA database are given in Table 2.

Table 2 The details and results of the methods related to the MURA database

Methods	**Number of Subjects**	Different Performance criteria (%)		
		Precision	Recall	F-Measure
Class 1	100	0.652	0.692	0.602
Class 2	293	0.663	0.683	0.613
Class 3	100	0.670	0.690	0.625
Class 4	100	0.688	0.708	0.632
Class 5	100	0.652	0.692	0.602

Conclusion

In this work, an efficient system for rapid and accurate diagnosis of bone fractures using CNP-based GP is proposed based on information gathered from X-ray images. As discussed, the feature generator in this work was created automatically and in the form of an evolved application. This was a distinct feature of the proposed model compared to the CNN model, which requires a lot of trial and error to build. Another advantage of the proposed model compared to CNN was its low operational complexity in the two phases of manufacturing and testing. To evaluate the performance of the proposed biometric system, the laboratory results on the MURA database confirmed its appropriate accuracy.

References

Al-Ayyoub, M., Hmeidi, I., & Rababah, H. (2013). Detecting Hand Bone Fractures in X-Ray Images. *Journal of Multimedia Processing and Technologies*, *4*(3), 155-168.

Al-Masni, M.A., Al-Antari, M.A., Park, J.M., Gi, G., Kim, T.Y., Rivera, P., & Kim, T.S. (2018). Simultaneous detection and classification of breast masses in digital mammograms via a deep learning YOLO-based CAD system. *Computer methods and programs in biomedicine, 157,* 85-94.

Bi, Y., Xue, B., & Zhang, M. (2019). An evolutionary deep learning approach using genetic programming with convolution operators for image classification. *In IEEE Congress on Evolutionary Computation (CEC)*, 3197-3204.

Ebsim, R., Naqvi, J., & Cootes, T.F. (2018). Automatic detection of wrist fractures from posteroanterior and lateral radiographs: a deep learning-based approach. *In International Workshop on Computational Methods and Clinical Applications in Musculoskeletal Imaging*, 114-125.

Gao, Z., Wang, D., He, X., & Zhang, H. (2018). Group-pair convolutional neural networks for multi-view based 3d object retrieval. *In Proceedings of the AAAI Conference on Artificial Intelligence*, *32*(1).

Guan, B., Yao, J., Zhang, G., & Wang, X. (2019). Thigh fracture detection using deep learning method based on new dilated convolutional feature pyramid network. *Pattern Recognition Letters*, *125*, 521-526.

Guan, B., Zhang, G., Yao, J., Wang, X., & Wang, M. (2020). Arm fracture detection in X-rays based on improved deep convolutional neural network. *Computers & Electrical Engineering*, *81*.

Ho-Le, T.P., Center, J.R., Eisman, J.A., Nguyen, T.V., & Nguyen, H.T. (2017). Prediction of hip fracture in post-menopausal women using artificial neural network approach. *In 39th Annual International Conference of the IEEE Engineering in Medicine and Biology Society (EMBC)*, 4207-4210.

Huang, G., Liu, Z., Van Der Maaten, L., & Weinberger, K.Q. (2017). Densely connected convolutional networks. *In Proceedings of the IEEE conference on computer vision and pattern recognition*, 4700-4708.

Ismael, S.A.A., Mohammed, A., & Hefny, H. (2020). An enhanced deep learning approach for brain cancer MRI images classification using residual networks. *Artificial intelligence in medicine, 102*.

Korfiatis, V.C., Tassani, S., & Matsopoulos, G.K. (2017). A new Ensemble Classification System for fracture zone prediction using imbalanced micro-CT bone morphometrical data. *IEEE journal of biomedical and health informatics, 22*(4), 1189-1196.

Li, X., Shen, L., Xie, X., Huang, S., Xie, Z., Hong, X., & Yu, J. (2020). Multi-resolution convolutional networks for chest X-ray radiograph based lung nodule detection. *Artificial intelligence in medicine, 103*.

Lindsey, R., Daluiski, A., Chopra, S., Lachapelle, A., Mozer, M., Sicular, S., & Potter, H. (2018). Deep neural network improves fracture detection by clinicians. *Proceedings of the National Academy of Sciences, 115*(45), 11591-11596.

Prihatini, R.S., Setyaningrum, A.H., & Shofi, I.M. (2017). Texture analysis and fracture identification of lower extremity bones X-ray images. *In 4th International Conference on Electrical Engineering, Computer Science and Informatics (EECSI)*, 1-5.

Qadir, Z., Ali, M., & Nesimoglu, T. (2018). Design and Development of a Low Cost Device for Bone Fracture Detection Using FFT Technique on MATLAB. *In 18th Mediterranean Microwave Symposium (MMS)*, 321-324.

Raghavendra, U., Bhat, N.S., Gudigar, A., & Acharya, U.R. (2018). Automated system for the detection of thoracolumbar fractures using a CNN architecture. *Future Generation Computer Systems, 85*, 184-189.

Tomita, N., Cheung, Y.Y., & Hassanpour, S. (2018). Deep neural networks for automatic detection of osteoporotic vertebral fractures on CT scans. *Computers in biology and medicine, 98*, 8-15.

Umadevi, N., & Geethalakshmi, S.N. (2012). Multiple classification system for fracture detection in human bone x-ray images. *In Third International Conference on Computing, Communication and Networking Technologies (ICCCNT'12)*, 1-8.

Wang, J. (2020). Anomaly Detection of Arm X-Ray Based on Deep Learning. *In IOP Conference Series: Earth and Environmental Science, 440*(4).

Wang, L., Cheng, H., Lan, H., Zheng, Y., & Li, K. (2016). Automatic recognition of pertrochanteric bone fractures in femur using level sets. *In 38th Annual International Conference of the IEEE Engineering in Medicine and Biology Society (EMBC)*, 3851-3854.

Yamada, A., Teramoto, A., Otsuka, T., Kudo, K., Anno, H., & Fujita, H. (2016). Preliminary study on the automated skull fracture detection in CT images using black-hat transform. *In 38th Annual International Conference of the IEEE Engineering in Medicine and Biology Society (EMBC)*, 6437-6440.

Singh, A.K., & Sharma, S.D. (2020). Digital Era in the Kingdom of Saudi Arabia: Novel Strategies of the Telecom Service Providers Companies. *Webology, 17*(1), 227-245.